

# Origin of hysteresis observed in association and dissociation of polymer chains in water

Yijie Lu,<sup>a</sup> Kejin Zhou,<sup>b</sup> Yanwei Ding,<sup>a</sup> Guangzhao Zhang<sup>\*a</sup> and Chi Wu<sup>ac</sup>

Received 14th September 2009, Accepted 18th November 2009

First published as an Advance Article on the web 10th February 2010

DOI: 10.1039/b918969f

By choosing poly(*N,N*-diethylacrylamide) which lacks the possibility to form intra- or inter-chain hydrogen bonds, we studied its chain association and dissociation in water by using laser light scattering (LLS), ultrasensitive differential scanning calorimetry (US-DSC) and Fourier transform infrared spectroscopy (FTIR). As the solution temperature increases, the average hydrodynamic radius ( $\langle R_h \rangle$ ) and average radius of gyration ( $\langle R_g \rangle$ ) decrease, indicating the intrachain shrinking. When the temperature is higher than its lower critical solution temperature (LCST,  $\sim 30$  °C), the apparent weight-average molar mass ( $M_{w,app}$ ) increases, reflecting the interchain association. At the same time, FTIR study reveals that as the temperature increases, the area ratio of two absorption peaks, respectively, associated to one hydrogen bonded carbonyl  $>C=O \cdots H-O-H$  and free carbonyl  $>C=O$  groups increases, while that related to two hydrated hydrogen bonded carbonyl groups decreases, indicating heating-induced dehydration. In the reversible cooling process,  $\langle R_h \rangle$ ,  $\langle R_g \rangle$ ,  $M_{w,app}$  and area ratios of the absorption peak are similar to those in the heating process for each given temperature, indicating that there is no hysteresis in the interchain association and dissociation. This present study confirms that the hysteresis previously observed for a sister polymer, poly(*N*-isopropylacrylamide), is due to the formation of some additional hydrogen bonds in its collapsed state at temperatures higher than the LCST.

## Introduction

The chain association and entanglement are important for understanding the structure–property relationships of polymer materials. Protein aggregation or association is also related to its function. There is increasing evidence that some diseases originate from protein association.<sup>1–5</sup> One noticeable event in macromolecular folding and association is the existence of a so-called hysteresis. Such a phenomenon has been observed in the re-naturation of some proteins.<sup>6,7</sup> Once a protein is denatured, it is normally difficult to reversibly fold to its original state, even under the same conditions. Hysteresis in polymer phase transitions has been studied for many years.<sup>8–17</sup> It has been observed in the sol–gel transition of the polysaccharide carrageenan,<sup>8</sup> the swelling/deswelling of polystyrene gels,<sup>9</sup> and phase transition of poly(lactic acid-*co*-glycolic acid)-*g*-poly(ethylene glycol) copolymer in aqueous solutions.<sup>10</sup> We have investigated the hysteresis in the coil-to-globule-to-coil transition and association-and-dissociation of poly(*N*-isopropylacrylamide) (PNIPAM) chains in water, which was attributed to some additional hydrogen bonds formed in

the collapsed state.<sup>11,12</sup> Later, we confirmed that such a hysteresis is indeed related to additional intrachain or interchain hydrogen bonds between carbonyl and amide groups, *i.e.*,  $>C=O \cdots H-N<$ , by using an ultrasensitive differential scanning calorimeter (US-DSC).<sup>13</sup> In parallel, Maeda *et al.*<sup>14</sup> investigated the phase transition of PNIPAM and poly(*N*-*n*-propylacrylamide) chains by use of FTIR. Their studies also demonstrated the formation of some intrachain and interchain hydrogen bonds. Van Mele *et al.*<sup>15–17</sup> studied the demixing and remixing of PNIPAM solution in water by modulated temperature differential scanning calorimetry and high-resolution ultrasonic spectroscopy. They showed that PNIPAM chains can recover the original conformation after a long time. However, it is not clear yet what exact role these additional hydrogen bonds play in the conformational changes and phase transitions of polymer chains in solution.

Poly(*N,N*-diethylacrylamide) (PDEAM) with a LCST of  $\sim 30$  °C has a similar structure to PNIPAM, but PDEAM chains are not able to form any hydrogen bonds by themselves.<sup>18–27</sup> Maeda *et al.*<sup>22</sup> used FTIR to study the dehydration of PDEAM as a function of temperature, but paid no attention to the hysteresis. Recently, we found that no hysteresis occurs in the coil-to-globule-to-coil transition of PDEAM individual chains.<sup>27</sup> In the present study, we prepared relatively narrowly distributed PDEAM chains. By using a combination of LLS, US-DSC and FTIR, we studied the phase transition of PDEAM in both the heating and cooling processes. In comparison with the previous results on PNIPAM chains, we attempt to elucidate the mechanism behind the hysteresis occurring in the interchain association and dissociation processes.

<sup>a</sup> Hefei National Laboratory for Physical Sciences at Microscale, Department of Chemical Physics, University of Science and Technology of China, Hefei, Anhui 230026, China.

E-mail: gzzhang@ustc.edu.cn; Fax: +86 (0)551 3606763; Tel: +86 (0)551 3606763

<sup>b</sup> Shanghai-Hong Kong Joint Laboratory in Chemical Synthesis, Shanghai Institute of Organic Chemistry, Chinese Academy of Science, 354 Fenglin Lu, Shanghai 200032, China

<sup>c</sup> Department of Chemistry, The Chinese University of Hong Kong, Shatin, N.T., Hong Kong

## Experimental

### Sample preparation

We prepared *N,N*-diethylacrylamide (DEA) by reacting acryloyl chloride with an excess of diethylamine in methylene chloride at 0 °C. The details can be found elsewhere.<sup>28</sup> The salt was removed by filtration and solvent was evaporated. The product was purified by three-time vacuum distillation, yielding a clear liquid that was kept in a freezer before use. The purified monomer, with 0.2 mol% azobisisobutyronitrile as initiator, was charged into a one-neck flask and then degassed by five cycles of freezing–pumping–thawing. The bulk polymerization was carried out at 25 °C for 30 days to yield a transparent solid. The resultant poly(*N,N*-diethylacrylamide) (PDEAM) was successively fractionated in a mixture of acetone and *n*-hexane (~1:2). In each cycle, the fraction with the highest molar mass was used for the next run. In this way, we successfully obtained a narrowly distributed PDEAM sample ( $M_w/M_n = 1.06$  and  $M_w = 1.7 \times 10^7$  g mol<sup>-1</sup>).

### Laser light scattering (LLS)

A commercial LLS spectrometer (ALV/DLS/SLS-5022F) equipped with a multi- $\tau$  digital time correlation (ALV5000) and a cylindrical 22-mW He–Ne laser ( $\lambda_0 = 632$  nm, UNIPHASE) as the light source was used. In static LLS, we were able to obtain both apparent weight-average molar mass ( $M_w$ ) and the  $z$ -averaged root-mean-square radius of gyration ( $\langle R_g^2 \rangle_z^{1/2}$ ) (or written as  $\langle R_g \rangle$ ) of polymer chains in a dilute solution from the angular dependence (15–150°) of the excess absolute time-averaged scattered intensity, *i.e.*, the Rayleigh ratio  $R_{vv}(q)$  by eqn (1):<sup>29</sup>

$$\frac{KC}{R_{vv}(q)} \cong \frac{1}{M_{w,app}} \left( 1 + \frac{1}{3} \langle R_g^2 \rangle q^2 \right) + 2A_2C \quad (1)$$

where  $K$  is a constant and  $q = (4\pi n/\lambda_0)\sin(\theta/2)$  with  $n$ ,  $\lambda_0$ ,  $\theta$  and  $A_2$  being the solvent refractive index, the wavelength of light in vacuum, the scattering angle and the second virial coefficient respectively. In the present study, the polymer concentration and  $A_2$  are so small that the  $2A_2C$  term can be neglected.<sup>27</sup>

In dynamic LLS,<sup>30,31</sup> the Laplace inversion of each measured intensity–intensity time correlation function  $G^{(2)}(q,t)$  in the self-beating mode can lead to a line-width distribution  $G(\Gamma)$ , where  $q$  is the scattering vector. For dilute solutions,  $\Gamma$  is related to the translational diffusion coefficient  $D$  by  $(\Gamma/q^2)_{C \rightarrow 0, q \rightarrow 0} \rightarrow D$ , so that  $G(\Gamma)$  can be converted into a translational diffusion coefficient distribution  $G(D)$  or further a hydrodynamic radius distribution  $f(R_h)$  via the Stokes–Einstein equation,  $R_h = (k_B T / 6\pi\eta_0) / D$ , where  $k_B$ ,  $T$  and  $\eta_0$  are the Boltzmann constant, the absolute temperature and the solvent viscosity, respectively.<sup>32,33</sup> In the current study, the PDEAM concentration used was  $1.0 \times 10^{-4}$  g mL<sup>-1</sup>.

### Ultra-sensitive differential scanning calorimeter (US-DSC)

US-DSC measurements were conducted on a VP-DSC micro-calorimeter from Microcal under an external pressure of 200 kPa with deionized water as the reference. The measured PDEAM solution and the reference solution were degassed at

25.0 °C for 30 min and equilibrated at 10 °C for 120 min before heating. In the cooling process, they were equilibrated at 70 °C for 120 min to eliminate the effect of thermal history. The concentration of PDEAM was 1.0 mg mL<sup>-1</sup>. Data analysis was done with Microcal software. The phase transition temperature ( $T_p$ ) was taken as that corresponding to the maximum excess specific heat capacity during the transition. The enthalpy change ( $\Delta H$ ) during the transition was calculated from the area under each peak.

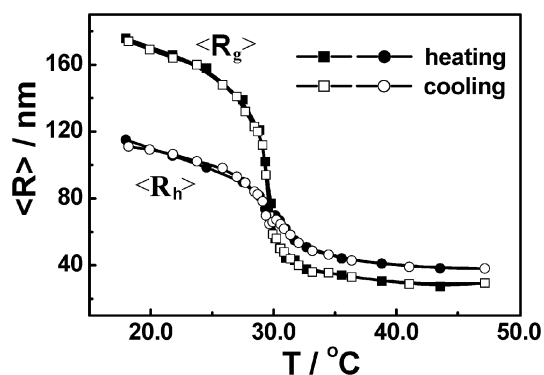
### FTIR measurements

A commercial Nicolet Magna 750 FTIR spectrometer with a 4 cm<sup>-1</sup> resolution was used. In a typical experiment, 10  $\mu$ L of PDEAM in D<sub>2</sub>O solution (2.0 wt%) was added to a cell between two KRS-5 crystals (diameter 32 mm, thickness 3.5 mm) with a space of 20  $\mu$ m. Here, we used D<sub>2</sub>O instead of H<sub>2</sub>O for FTIR experiments because the bending mode of D<sub>2</sub>O moves to 1200 cm<sup>-1</sup>, preventing its band overlapping with the amide I band. The IR cell was thermally controlled. An electronic thermometer with a precision of  $\pm 0.1$  °C was used to continuously monitor the cell temperature.

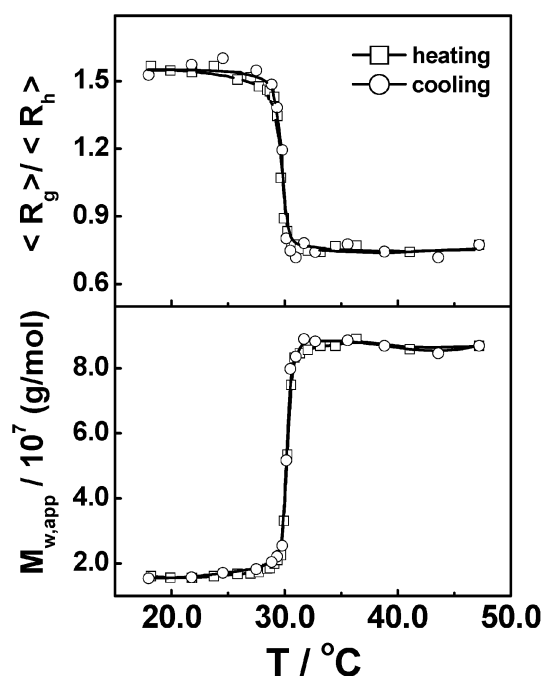
## Results and discussion

Fig. 1 shows the temperature dependence of  $\langle R_g \rangle$  and  $\langle R_h \rangle$  of PDEAM chains in one heating-and-cooling cycle, where each data point was obtained after the system reached the equilibrium; that is, there were no further changes in  $\langle R_g \rangle$  or  $\langle R_h \rangle$ . As the temperature increases, both  $\langle R_g \rangle$  and  $\langle R_h \rangle$  decrease before the temperature reaches 29.6 °C, whereas the apparent molar mass ( $M_{w,app}$ ) remains constant, as shown in Fig. 2, indicating the intrachain contraction of individual PDEAM chains. In the range 29.6–30.9 °C,  $M_{w,app}$  sharply increases, accompanied by moderate increases of  $\langle R_g \rangle$  and  $\langle R_h \rangle$ , clearly signalling the interchain association. When the temperature is higher than 30.9 °C, both  $\langle R_g \rangle$  and  $\langle R_h \rangle$  slightly decrease with the temperature but  $M_{w,app}$  levels off, suggesting that the intrachain contraction is still undergoing inside each aggregate even after the interchain association ceases. Finally,  $\langle R_g \rangle$  and  $\langle R_h \rangle$  level off at 29 nm and 38 nm, respectively. Note that the multi-chain aggregates are even smaller than individual initial chains in their expanded coil state, revealing that the intrachain contraction dominates the interchain association. In the cooling process, as the temperature decreases to LCST, both  $\langle R_g \rangle$  and  $\langle R_h \rangle$  increase, but  $M_{w,app}$  sharply decreases, indicating the swelling and quick dissociation of the aggregates into individual chains. It is important to note that the absence of hysteresis implies a much weaker segment–segment interaction in PDEAM than in PNIPAM.

Fig. 2 shows the temperature dependence of  $\langle R_g \rangle / \langle R_h \rangle$  for PDEAM chains in water. It is known that  $\langle R_g \rangle / \langle R_h \rangle$  reflects the conformation of a polymer chain or the density distribution in space. For a uniform non-draining sphere, hyper-branched cluster or random coil,  $\langle R_g \rangle / \langle R_h \rangle \sim 0.774$ , 1.0–1.2, and 1.5–1.8, respectively.<sup>34–37</sup> Here,  $\langle R_g \rangle / \langle R_h \rangle \sim 1.6$  when the temperature is lower than the LCST in either the heating or cooling process, indicating that PDEAM chains are extended random coils. In the heating process, as the temperature increases from 28.3 °C to 30.9 °C,  $\langle R_g \rangle / \langle R_h \rangle$  decreases from



**Fig. 1** Temperature dependence of average hydrodynamic radius ( $\langle R_h \rangle$ ) and average radius of gyration ( $\langle R_g \rangle$ ) of PDEAM chains in water in one heating-and-cooling cycle.



**Fig. 2** Temperature dependence of the ratio of average radius of gyration to average hydrodynamic radius ( $\langle R_g \rangle / \langle R_h \rangle$ ) and apparent weight-average molar mass ( $M_{w,app}$ ) of PDEAM chains in water in one heating-and-cooling cycle.

$\sim 1.6$  to  $\sim 0.76$ , revealing that the random-coil-like chains collapse and associate to form interchain aggregates with a relatively uniform density.<sup>12</sup> In contrast, as the solution is cooled from 30.9 °C to 28.3 °C,  $\langle R_g \rangle / \langle R_h \rangle$  changes back from  $\sim 0.76$  to  $\sim 1.6$  due to chain swelling and dissociation from interchain aggregates. On the other hand, it is known that PNIPAM in water has a hysteresis in its conformational change and in its interchain association/dissociation, attributable to the formation of additional hydrogen bonds in their collapsed state.<sup>12,13,38,39</sup> The investigation on the association/dissociation of PNIPAM chains in water by FTIR reveals that some of the additional hydrogen bonds formed at higher temperatures remain during the cooling process even at a temperature below the LCST.<sup>12</sup> A comparison between PNIPAM and PDEAM indicates that the hysteresis originates

from some additional hydrogen bonds formed in their collapsed state at temperatures higher than the LCST.

To further elucidate the origin of the hysteresis observed for PNIPAM in water, we also examined the association and dissociation kinetics of PDEAM in water after a temperature jump, which can reveal more details of the intrachain contraction and interchain association. Fig. 3 shows the time dependence of apparent weight-average molar mass ( $M_{w,app}$ ) and average hydrodynamic radius ( $\langle R_h \rangle$ ) after a temperature jump from 18.0 °C to 30.7 °C. All the data were obtained as soon as the sample cell was placed in the scattering cell with the final temperature. Note that the final temperature (30.7 °C) is only slightly higher than the LCST ( $\sim 30$  °C), which leads to a slow association. The changes of  $M_{w,app}$  and  $\langle R_h \rangle$  can be divided into three regions. In Region I (0–9.4 min),  $M_{w,app}$  increases but  $\langle R_h \rangle$  decreases, indicating that both intrachain contraction and interchain association occur. In Region II (9.4–56.6 min), the interchain association is dominant so that both  $M_{w,app}$  and  $\langle R_h \rangle$  increase. In Region III ( $> 56.6$  min), both  $M_{w,app}$  and  $\langle R_h \rangle$  level off, indicating that the intrachain contraction and interchain association cease.

Fig. 4 shows the time dependence of  $M_{w,app}$  and  $\langle R_h \rangle$  when the solution is quenched from 40.0 °C to 29.6 °C. In the first 15 min,  $M_{w,app}$  decreases but  $\langle R_h \rangle$  increases, indicating the chain swelling and the dissociation of the interchain aggregates. Afterwards, both  $M_{w,app}$  and  $\langle R_h \rangle$  slightly change, indicating that all the aggregates have dissociated into individual chains. In other words, each PDEAM aggregate directly and quickly dissociates back into individual chains when the solution is cooled to a temperature below the LCST. This is different from the dissociation of PNIPAM aggregates in which some aggregates are not able to completely dissociate

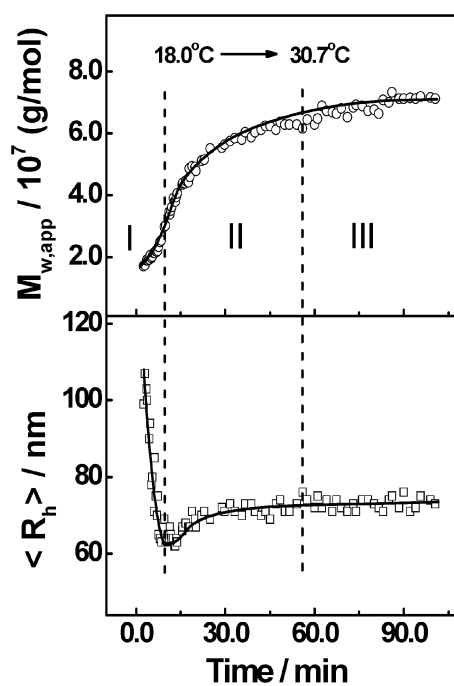


**Fig. 3** Time dependence of apparent weight-average molar mass ( $M_{w,app}$ ) and average hydrodynamic radius ( $\langle R_h \rangle$ ) of PDEAM chains in water after a temperature jump from 18.0 °C to 30.7 °C.

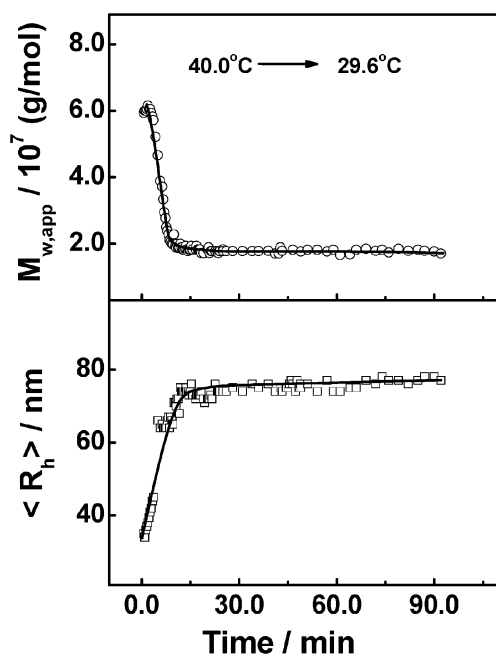


**Fig. 4** Time dependence of apparent weight-average molar mass ( $M_{w,app}$ ) and average hydrodynamic radius ( $\langle R_h \rangle$ ) of PDEAM chains in water after the solution is quenched from 40.0 °C to 29.6 °C.

back into individual chains even when the solution temperature is kept at 25 °C for a long time. Namely, some of additional hydrogen bonds formed in the collapsed state cannot be removed so that they make each PNIPAM aggregate behave like a “microgel”.<sup>12</sup> Actually, it takes a long time for PNIPAM to recover its original conformation.<sup>17</sup> Clearly, the dissociation of chain aggregates does not exhibit a hysteresis when no additional hydrogen bonds form in the collapsed state. To further confirm such a hydrogen-bonding origin, we also investigated the thermally induced association and dissociation of PDEAM in water by using US-DSC and FTIR.

Fig. 5 shows the temperature dependence of the specific heat capacity ( $C_p$ ) of PDEAM solution at different heating rates. The thermograms are endothermic and asymmetric with a sharp increase and a gradual decrease of heat capacity at a temperature below and above the phase transition temperature ( $T_p$ ), respectively. In comparison with PNIPAM chains,<sup>13</sup> PDEAM chains exhibit a much broader phase transition, and the heat capacity at  $T_p$  for PDEAM is about 5 times lower than that for PNIPAM. Actually, such a broad transition peak was observed before in poly(*N*-vinylcaprolactam) which cannot form additional hydrogen bonds.<sup>40</sup> Therefore, the absence of additional hydrogen bonds is responsible for the broad transition. Fig. 5 also shows that  $T_p$  increases with the heating rate. As stated before,<sup>41</sup> this is because the chain contraction and association cannot follow the temperature change. In other words, the phase transition occurring at a certain heating rate is not in thermodynamic equilibrium. Particularly, a bimodal transition is observed when the heating rate is lower than 0.83 °C min<sup>-1</sup>. As the LLS studies above revealed, only intrachain contraction occurs at a temperature below the phase transition temperature, whereas both

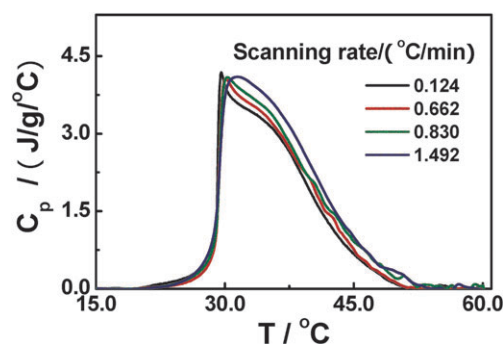


**Fig. 5** Temperature dependence of specific heat capacity ( $C_p$ ) of PDEAM chains at different heating rates.

interchain association and intrachain contraction happen at a temperature above the phase transition temperature. The bimodal transition reflects the intrachain contraction and interchain association which do not occur simultaneously. Actually, as the heating rate increases over 0.83 °C min<sup>-1</sup>, the bimodal transition gradually turns into a unimodal one with  $T_p$  shifting to a higher temperature. This is because PDEAM chains do not have time to contract at a lower temperature in a quick heating, and the intrachain contraction and interchain association almost simultaneously happen at a higher temperature. Note that such a transition was not observed for PNIPAM chains in the heating process.<sup>13,42</sup> This is probably because the additional hydrogen bonding in PNIPAM leads the intrachain contraction and interchain association to happen at a similar rate.

Fig. 6 shows the temperature dependence of the specific heat capacity ( $C_p$ ) of PDEAM solution at different cooling rates. Clearly,  $T_p$  decreases with the cooling rate, indicating the dissolution of the collapsed PDEAM chains also cannot follow the temperature change. A bimodal transition is observed in the cooling process. As we know, PNIPAM chains exhibit a bimodal transition in the cooling process since the dissolution of PNIPAM aggregates involves the disruption of additional hydrogen bonds and the dissolution of the collapsed chains.<sup>13</sup> Considering that no additional hydrogen bonds form in PDEAM chains, the reason for the bimodal transition of PDEAM chains should be different. As discussed above, the intrachain contraction and interchain association of PDEAM chains usually do not occur simultaneously, indicating the difference between the intrachain and interchain interaction. In the cooling process, the dissociation of the chain aggregates and swelling of the chains depend upon the destruction of the interchain and intrachain interaction, respectively. Their difference leads the two processes to separate. That is why we can observe a bimodal transition in PDEAM chains.

Fig. 7 shows the scanning rate dependence of transition temperature ( $T_p$ ) of PDEAM chains.  $T_p$  linearly increases with the heating rate, indicating that the intrachain contraction and interchain association are dependent on the heating rate because they cannot follow the temperature change. In contrast, the decrease of  $T_p$  with cooling rate indicates the dissociation of the collapsed PDEAM chains also cannot follow the temperature change.  $T_p$  is around 29.6 °C in

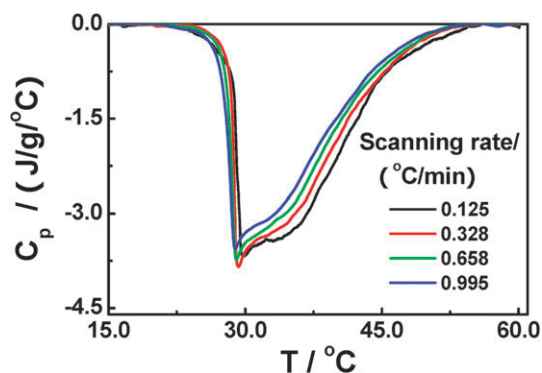


Fig. 6 Temperature dependence of the specific heat capacity ( $C_p$ ) of PDEAM chains at different cooling rates.

either heating or cooling process when the scanning rate is lower than  $0.13\text{ °C min}^{-1}$ , clearly indicating no hysteresis in the association and dissociation of PDEAM chains. When the scanning rate is higher than  $0.13\text{ °C min}^{-1}$ , a difference between  $T_p$  values in heating and cooling process can be observed, which increases with the scanning rate. As discussed above, the phase transition occurring at a certain heating rate is far from the thermodynamic equilibrium. Such a difference at high scanning rate is the result of kinetic effect.

Fig. 7 also shows that the enthalpy change ( $\Delta H$ ) increases with the heating rate. A similar behaviour has been reported about PNIPAM chains before.<sup>13,41,43</sup> Our LLS studies on PDEAM chains reveal that a fast heating leads to smaller aggregates or more intrachain contraction. Since intrachain contraction involves a larger change in the chain conformation and the chain collapse induces more stress inside, the energy required for the intrachain contraction is higher than that for interchain interaction. That is why a fast heating leads to a larger  $\Delta H$ . In the cooling process, the aggregates are dissolved gradually from the outer layer to the core with the destruction

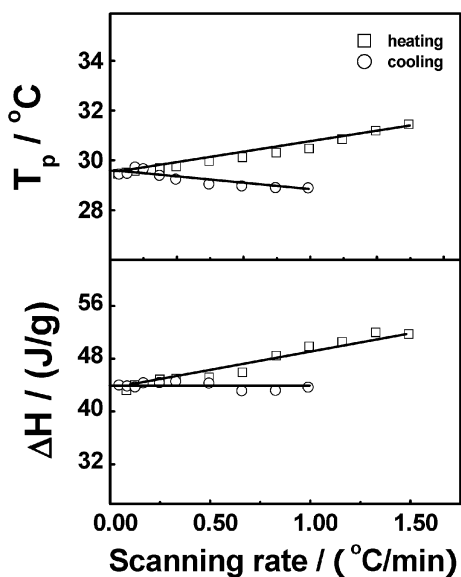


Fig. 7 Scanning rate dependence of transition temperature ( $T_p$ ) and enthalpy change ( $\Delta H$ ) of PDEAM chains.

of the interchain and intrachain interactions.  $\Delta H$  associated with the dissolution is mainly controlled by the cooperative diffusion of the chains in water. Therefore, the  $\Delta H$  value is nearly independent of the cooling rate. A similar phenomenon has also been observed in the dissociation of PNIPAM aggregates and the denaturation of some proteins.<sup>13,44</sup> Fig. 7 shows that  $\Delta H$  values in heating and cooling process at a scanning rate below  $0.13\text{ °C min}^{-1}$  are almost equal. Actually, the extrapolation of  $\Delta H$  or  $T_p$  to zero scanning rate yields the enthalpy change ( $\Delta H_0$ ) and phase transition temperature ( $T_{p,0}$ ) in equilibrium state. Clearly, both heating and cooling lead to the same  $\Delta H_0$  and  $T_{p,0}$ . In contrast,  $\Delta H_0$  and  $T_{p,0}$  for PNIPAM chains in heating process are different from those in cooling process due to the additional hydrogen bonds.<sup>13</sup> The facts further indicate that the hysteresis arises from the additional hydrogen bonds.

Fig. 8 shows FTIR spectra of PDEAM in  $D_2O$  in the range of  $1660\text{--}1560\text{ cm}^{-1}$  at different temperatures. A multi-peak fitting leads to the division of the amide I band into three peaks, centered at  $1638$ ,  $1619$  and  $1599\text{ cm}^{-1}$ , respectively. As reported before,<sup>22</sup> the band at  $1619$  and  $1599\text{ cm}^{-1}$  are associated with the carbonyl  $>C=O$  groups coupled with one and two water molecules. The band at  $1638\text{ cm}^{-1}$  is assigned to free carbonyl  $>C=O$  groups without hydrogen bonding because it is close to  $1637\text{ cm}^{-1}$  observed for solid PDEAM. Furthermore, Fig. 9 shows that the curves at  $28\text{ °C}$  in the heating and cooling processes are nearly identical, quite different from those at  $46\text{ °C}$ , revealing that the carbonyl  $>C=O$  group is coupled with water molecules *via* some hydrogen bonds when the solution temperature is lower than the LCST. Assuming that each hydrogen bond contributes a similar intensity in the spectrum, we can estimate the degree of dehydration and the fractions of intra- and inter-chain hydrogen bonds from the area ratio of peaks obtained from a multi-peak fitting.

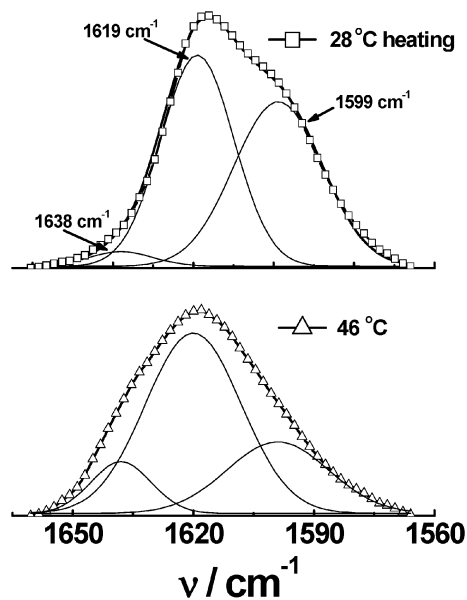
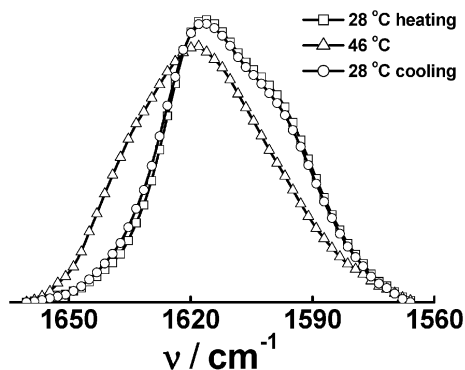
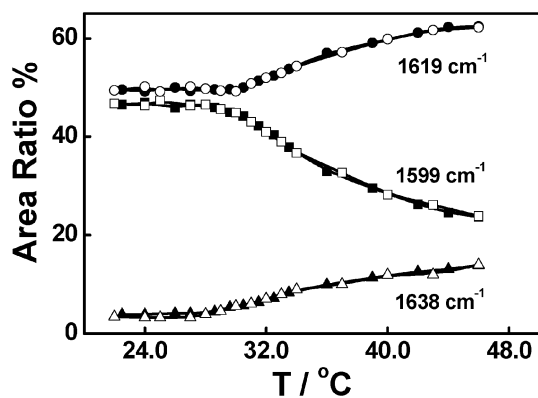


Fig. 8 FTIR spectra of 2.0 wt% PDEAM chains in  $D_2O$  with the baseline of amide I band subtracted at  $28\text{ °C}$  and  $46\text{ °C}$  in heating process, respectively.



**Fig. 9** FTIR spectra of 2.0 wt% PDEAM chains in D<sub>2</sub>O with the baseline of amide I band subtracted at 28 °C in heating process, 46 °C and 28 °C in cooling process, respectively.



**Fig. 10** Temperature dependence of relative areas of the three peaks in the amide I band of PDEAM chains in D<sub>2</sub>O, where open and filled symbols represent data obtained in the heating and cooling processes, respectively.

Fig. 10 shows the temperature dependence of the area ratio ( $R_{\text{peak}}$ ) of three different hydrogen bonds in one heating-and-cooling cycle. As the temperature increases, the area ratio for the peak at 1638 cm<sup>-1</sup> ( $R_{\text{peak},1638}$ ) increases when  $T > \text{LCST}$  and reaches a plateau, indicating that free carbonyl  $>\text{C}=\text{O}$  groups weighs more and the dehydration occurs. On the other hand, the area ratio for the peak at 1599 cm<sup>-1</sup> ( $R_{\text{peak},1599}$ ) decreases during the heating, presumably due to a partial dehydration. In addition, the increase of the area ratio for the peak at 1619 cm<sup>-1</sup> ( $R_{\text{peak},1619}$ ) with the temperature suggests that the carbonyl  $>\text{C}=\text{O}$  group coupled with two water molecules are easier to undergo the dehydration than those coupled with only one water molecule. This is consistent with our LLS results. It is known that for PNIPAM, the hydrogen bonds ( $>\text{C}=\text{O}\cdots\text{H}-\text{N}$ ) cannot be completely removed, even at temperatures lower than its LCST.<sup>12</sup> For PDEAM, no intra- or interchain hydrogen bond can be formed even at the collapsed state so that the carbonyl  $>\text{C}=\text{O}$  groups only form hydrogen bonds with water molecules at temperatures lower than its LCST, resulting in no hysteresis.

## Conclusions

By choosing poly(*N,N*-diethylacrylamide) (PDEAM), without any possibility to form intra- and inter-chain hydrogen bonds,

we studied its thermally induced chain association and dissociation in water. The Fourier transform infrared spectroscopy (FTIR) study reveals that each carbonyl  $>\text{C}=\text{O}$  group on PDEAM can associate with one or two water molecules *via* hydrogen bonding, depending on whether the solution temperature is higher or lower than its lower critical solution temperature (LCST,  $\sim 30$  °C). The laser light scattering (LLS) study shows no hysteresis between the association and dissociation of PDEAM chains in water during one heating-and-cooling cycle. Besides, the association and dissociation of PDEAM in water are either intrachain dominant or interchain dominant, depending on whether the solution temperature is lower or higher than LCST. The US-DSC study shows that phase transition temperature and the enthalpy change in heating and cooling process are almost equal at a low scanning rate. The current study confirms that the hysteresis previously observed for a sister polymer, poly(*N*-isopropylacrylamide) (PNIPAM), is due to the formation of additional intra- and inter-chain hydrogen bonds in the collapsed state at temperatures higher than its LCST.

## Acknowledgements

The financial support of Ministry of Science and Technology of China (2007CB936401), the National Natural Scientific Foundation of China (NNSFC) Projects (20534020 and 20574065) and the Hong Kong Special Administration Region (HKSAR) Earmarked Project (CUHK4046/08P, 2160365) is gratefully acknowledged.

## References

- 1 M. Fändrich, M. A. Fletcher and C. M. Dobson, *Nature*, 2001, **410**, 165.
- 2 C. M. Dobson, *Nature*, 2003, **426**, 884.
- 3 A. L. Goldberg, *Nature*, 2003, **426**, 895.
- 4 D. J. Selkoe, *Nature*, 2003, **426**, 900.
- 5 F. E. Cohen and J. W. Kelly, *Nature*, 2003, **426**, 905.
- 6 A. Fuchs, C. Seiderer and R. Seckler, *Biochemistry*, 1991, **30**, 6598.
- 7 B. Schuler, R. Rachel and R. Seckler, *J. Biol. Chem.*, 1999, **274**, 18589.
- 8 D. A. Rees, I. W. Steele and F. B. Williamson, *J. Polym. Sci., Part C: Polym. Symp.*, 1969, **28**, 261.
- 9 J. M. O'Kane and D. C. Sherrington, *Macromolecules*, 1990, **23**, 5286.
- 10 B. Jeong, C. F. Windisch, Jr, M. J. Park, Y. S. Sohn, A. Gutowska and K. Char, *J. Phys. Chem. B*, 2003, **107**, 10032.
- 11 C. Wu and X. H. Wang, *Phys. Rev. Lett.*, 1998, **80**, 4092.
- 12 H. Cheng, L. Shen and C. Wu, *Macromolecules*, 2006, **39**, 2325.
- 13 Y. W. Ding, X. D. Ye and G. Z. Zhang, *Macromolecules*, 2005, **38**, 904.
- 14 Y. Maeda, T. Nakamura and I. Ikeda, *Macromolecules*, 2001, **34**, 1391.
- 15 K. Van Durme, L. Delellio, E. Kudryashov, V. Buchin and B. Van Mele, *J. Polym. Sci., Part B: Polym. Phys.*, 2005, **43**, 1283.
- 16 K. Van Durme, H. Rahier and B. Van Mele, *Macromolecules*, 2005, **38**, 10155.
- 17 K. Van Durme, G. Van Assche and B. Van Mele, *Macromolecules*, 2004, **37**, 9596.
- 18 R. Freitag, T. Baltes and M. Eggert, *J. Polym. Sci., Part A: Polym. Chem.*, 1994, **32**, 3019.
- 19 M. Kobayashi, T. Ishizone and S. Nakahama, *Macromolecules*, 2000, **33**, 4411.
- 20 H. G. Schild and D. A. Tirrell, *J. Phys. Chem.*, 1990, **94**, 4352.
- 21 D. G. Lessard, M. Ousalem and X. X. Zhu, *Can. J. Chem.*, 2001, **79**, 1870.

- 22 Y. Maeda, T. Nakamura and I. Ikeda, *Macromolecules*, 2002, **35**, 10172.
- 23 M. Itakura, K. Inomata and T. Nose, *Polymer*, 2000, **41**, 8681.
- 24 H. Y. Liu and X. X. Zhu, *Polymer*, 1999, **40**, 6985.
- 25 J. Spěváček, D. Geschke and M. Ilavský, *Polymer*, 2001, **42**, 463.
- 26 D. G. Lessard, M. Ousalem, X. X. Zhu, A. Eisenberg and P. J. Carreau, *J. Polym. Sci., Part B: Polym. Phys.*, 2003, **41**, 1627.
- 27 K. J. Zhou, Y. J. Lu, J. F. Li, L. Shen, G. Z. Zhang, Z. W. Xie and C. Wu, *Macromolecules*, 2008, **41**, 8927.
- 28 I. Idziak, D. Avoce, D. Lessard, D. Gravel and X. X. Zhu, *Macromolecules*, 1999, **32**, 1260.
- 29 B. H. Zimm, *J. Chem. Phys.*, 1948, **16**, 1099.
- 30 R. Pecora, *Dynamic Light Scattering*, Plenum Press, New York, 1976.
- 31 B. Chu, *Laser Light Scattering*, Academic Press, New York, 2nd edn, 1991.
- 32 C. Wu and K. Q. Xia, *Rev. Sci. Instrum.*, 1994, **65**, 587.
- 33 S. W. Provencher, *J. Chem. Phys.*, 1976, **64**, 2772.
- 34 S. W. Provencher, *Biophys. J.*, 1976, **16**, 27.
- 35 I. Teraoka, *Polymer Solutions*, John Wiley & Sons, New York, 2002.
- 36 W. Burchard, in *Light Scattering Principles and Development*, ed. W. Brown, Clarendon Press, Oxford, 1996.
- 37 W. Burchard, M. Schmidt and W. H. Stockmayer, *Macromolecules*, 1980, **13**, 1265.
- 38 X. H. Wang, X. P. Qiu and C. Wu, *Macromolecules*, 1998, **31**, 2972.
- 39 G. M. Liu and G. Z. Zhang, *J. Phys. Chem. B*, 2005, **109**, 743.
- 40 A. Laukkanen, L. Valtola, F. M. Winnik and H. Tenhu, *Macromolecules*, 2004, **37**, 2268.
- 41 N. V. Grinberg, A. S. Dubovik, V. Y. Grinberg, D. V. Kuznetsov, E. E. Makhaeva, A. Y. Grosberg and T. Tanaka, *Macromolecules*, 1999, **32**, 1471.
- 42 Y. W. Ding, X. D. Ye and G. Z. Zhang, *J. Phys. Chem. B*, 2008, **112**, 8496.
- 43 V. Y. Grinberg, A. S. Dubovik, D. V. Kuznetsov, N. V. Grinberg, A. Y. Grosberg and T. Tanaka, *Macromolecules*, 2000, **33**, 8685.
- 44 V. Y. Grinberg, T. V. Burova and T. Haertléand V. B. Tolstoguzov, *J. Biotechnol.*, 2000, **79**, 269.